Beyerle, G. (2009): Carrier phase wind-up in GPS reflectometry. - GPS Solutions, 13, 3, 191-198

DOI: 10.1007/s10291-008-0112-1

GPS Solutions manuscript No.
(will be inserted by the editor)

Carrier phase wind-up in GPS reflectometry

G. Beyerle

GFZ German Research Centre for Geosciences, Potsdam, Germany

Received: XXX / Revised version: XXX

Abstract Changes in GPS transmitter and receiver antenna orientations induce variations in observed carrier phase values. An analytic formula for this well-known carrier phase wind-up correction is derived which generalizes a previous result. In addition, it is shown that in GPS reflectometry the wind-up values of direct and coherently reflected rays may differ by up to several centimeters. The results are discussed on the basis of simulated measurements.

1 Introduction

Global Positioning System (GPS) satellites transmit L-band signals which are right-hand circularly polarized (RHCP) (see, e.g., *Misra and Enge*, 2006). The measured carrier phase, therefore, varies when the receiving and/or transmitting antennas change their relative orientations. This effect is known as carrier phase wind-up and has been thoroughly discussed by

Wu et al. (1993). In general, the fractional part of the carrier phase wind-up constitutes a minor correction on the order of a few centimeters in terms of phase path, but needs to be corrected for in high-precision applications or other specific utilizations (*Wu et al.*, 1993; *Tetewsky and Mullen*, 1997; *Kim et al.*, 2006; *Beutler et al.*, 2007; *García-Fernández et al.*, 2008). The integer part may accumulate with time and is estimated by comparing the wind-up value at the current and preceding epoch (*Wu et al.*, 1993). In the following, the integer part of the wind-up value is ignored and I consider only its value modulo 2π, i.e., its fractional part.

The GPS satellites orbit the Earth at altitudes of about 20,180 km and their signals propagate to ground-based receivers at transmitter antenna off-boresight angles between 0° (satellite in the receiver's zenith) and about 13.9° (satellite at the receiver's horizon). Even for space-borne receivers placed in low-Earth orbits at altitudes below 2000 km, the transmitter off-boresight angle remains below 18.4°.

It is well known that for non-zero off-boresight angles the GPS signals' polarization state at the receiver antenna phase center deviates from pure RHCP (*Wu et al.*, 1993). Still, the left-hand circularly polarized (LHCP) power levels are small compared to the RHCP levels. For most practical purposes they are negligible and the assumption of a pure RHCP transmitter signal (equation (3) in *Wu et al.* (1993)) is well justified. As will be shown in the following, the error in carrier phase wind-up introduced by this approximation lies in the sub-millimeter range in terms of phase

path. In GPS reflectometry, however, the phase wind-up correction of a coherently reflected signal differs by up to several centimeters from the value experienced by the direct signal and needs to be taken into account for the determination of altimetric heights.

The paper is organized as follows. The next section reviews the derivation of the carrier phase wind-up for direct rays and derives a generalization of the phase wind-up expression given by *Wu et al.* (1993). The subsequent section focuses on the phase wind-up calculation of reflected rays taking into account the change of polarization state at the reflecting surface. Finally, the results are discussed using simulated measurements.

2 Theory

In the following discussion the transmitted signal is taken to be the superposition of a RHCP and LHCP component. That is, the signal is perfectly polarized and contains no unpolarized contributions. Furthermore, it is assumed that both, the transmitter and the receiver antenna, may be modelled as crossed dipoles (*Wu et al.*, 1993). A crossed dipole consists of two short dipoles oriented perpendicular to each other. The aligned dipole (superscript a) and the transverse dipole (superscript t) are identical except that the signal path to the transverse dipole adds an additional phase delay of $\pi/2$. In addition, the model assumes that the antenna's phase center coincides with the crosspoint of the aligned and transverse dipole. Phase center variations, which may assume values of several centimeters for real

GPS antennas, are not taken into account (e.g., *Schmid et al.*, 2007; *Montenbruck et al.*, 2008). Furthermore, atmospheric and ionospheric effects on the signal's carrier phase are ignored as well.

The transmitter antenna orientation is characterized by two unit vectors, $\hat{t}^a$ and $\hat{t}^t$. The symbol $\hat{t}^a$ $\left(\hat{t}^t\right)$ denotes the unit vector in the direction of the aligned (transverse) dipole. The antenna boresight direction is given by $\hat{t}^b \equiv \hat{t}^a \times \hat{t}^t$ and the vectors $[\hat{t}^a, \hat{t}^t, \hat{t}^b]$ form a right-hand, orthonormal coordinate system. Similarly, the receiver's antenna orientation is described by the three unit vectors $[\hat{r}^a, \hat{r}^t, \hat{r}^b]$ with $\hat{r}^b \equiv \hat{r}^a \times \hat{r}^t$. The vectors $\hat{t}^b$ and $\hat{r}^b$ point towards the transmitter and receiver antennas' top sides, respectively.

2.1 Phase Wind-up for Direct Rays

The electric field $\mathbf{E}^a(\Omega)$ generated by the aligned dipole at a location $\mathbf{r}$ far away from the transmitter antenna is (e.g., *Jackson*, 1999)

$$\begin{aligned} \mathbf{E}^a(\Omega) &\approx \frac{1}{4\pi\,\epsilon_0}\,\left[\frac{\omega^2}{c^2\,r^3}\,(\mathbf{r}\times\mathbf{p})\times\mathbf{r}\right]\,\cos(\omega\,t-\mathbf{k}\cdot\mathbf{r}-\delta) \\ &\propto \left((\hat{k}\times\hat{t}^a)\times\hat{k}\right)\,\cos(\Omega) \end{aligned} \tag{1}$$

where $\Omega \equiv \omega\,t - \mathbf{k}\cdot\mathbf{r} - \delta$. Here, ω and t denote the signal's angular frequency and time, $\mathbf{r}$ is the difference vector between the receiver and transmitter phase centers, $\mathbf{k} \equiv \hat{k}\,2\pi/\lambda$ is the wave vector with $\hat{k} \equiv \mathbf{k}/|\mathbf{k}|$, $\mathbf{p}$ is the dipole moment, ϵ_0 is the permittivity of free space, c is the velocity of light and δ is an additional phase offset. The far-field approximation (1) is valid provided that $|\mathbf{r}|\,\omega/c \gg 1$.

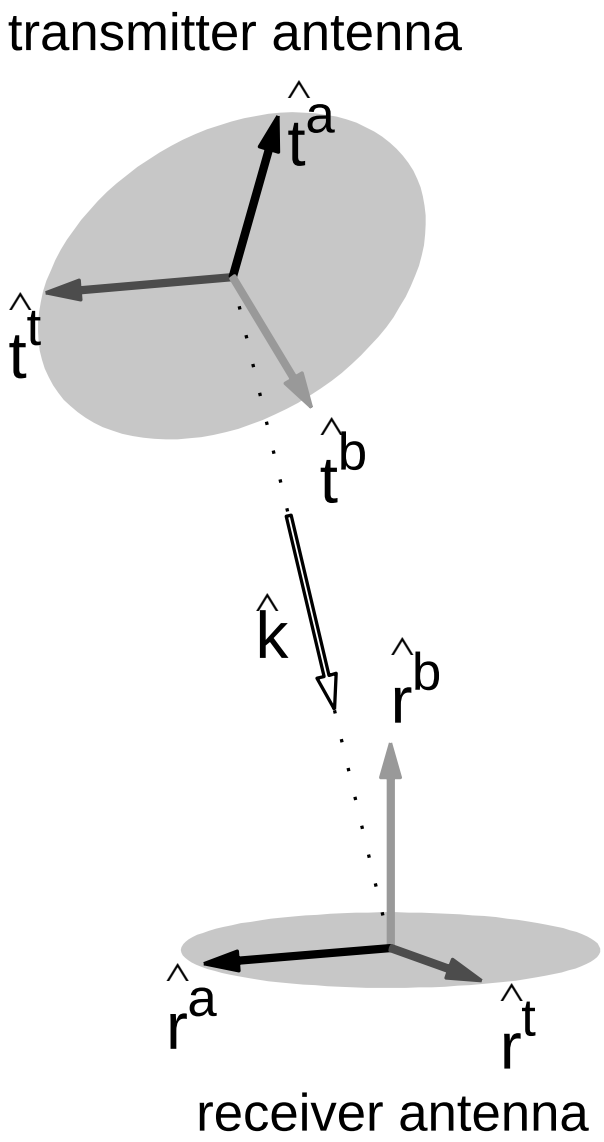

Fig. 1 Transmitter and receiver antenna geometry. The arrows mark the aligned and transverse dipoles' directions as well as the antenna boresight directions. $\hat{k}$ is the normalized wave vector.

The present analysis concentrates on phase changes induced by the antenna orientations; phase variations caused by the relative motion between the two antenna phase centers are disregarded and $|\mathbf{r}|$ is considered constant. Since the absolute value of the electric field amplitudes are irrelevant for the present discussion, the constant of proportionality in (1) (and analogous expressions below) will be set to unity without loss of generality.

The transverse dipole transmits a signal which is delayed by $\pi/2$ with respect to the signal transmitted by the aligned dipole and the corresponding field is proportional to

$$\mathbf{E}^t(\Omega) \propto \left((\hat{k} \times \hat{t}^t) \times \hat{k}\right) \sin(\Omega) \tag{2}$$

The overall field $\mathbf{E}(\Omega)$ is the superposition of $\mathbf{E}^a(\Omega)$ and $\mathbf{E}^t(\Omega)$, i.e.

$$\begin{aligned} \mathbf{E}(\Omega) &\equiv \mathbf{E}^a(\Omega) + \mathbf{E}^t(\Omega) \\ &\propto \mathbf{T}^a(\hat{k}) \cos(\Omega) + \mathbf{T}^t(\hat{k}) \sin(\Omega) \end{aligned} \tag{3}$$

where

$$\begin{aligned} \mathbf{T}^a(\hat{k}) &\equiv \left(\hat{k} \times \hat{t}^a\right) \times \hat{k} \\ \mathbf{T}^t(\hat{k}) &\equiv \left(\hat{k} \times \hat{t}^t\right) \times \hat{k} \end{aligned} \tag{4}$$

and the fact is used that the constants of proportionality in (1,2) are identical.

Following *Wu et al.* (1993) the open-circuit voltage V^a at the aligned receiver dipole is proportional to

$$V^a \propto \hat{r}^a \cdot \mathbf{E}(\Omega) \tag{5}$$

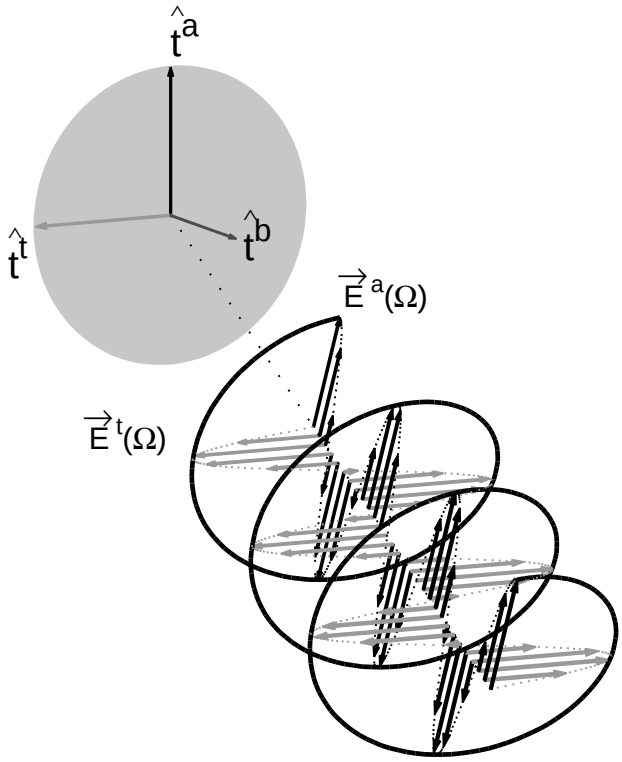

Fig. 2 The electric fields $\mathbf{E}^a(\Omega)$ and $\mathbf{E}^t(\Omega)$ transmitted towards direction $\hat{k}$ by two dipoles oriented at $\hat{t}^a$ and $\hat{t}^t$. Note that $\mathbf{E}^a(\Omega)$ and $\mathbf{E}^t(\Omega)$ are perpendicular to each other only if $\hat{t}^a \perp \hat{k}$ or $\hat{t}^t \perp \hat{k}$.

Analogous to the transmitting transverse dipole, the receiving transverse dipole's signal path inserts a phase shift of $\pi/2$ and the corresponding voltage V^t is given by

$$V^t \propto \hat{r}^t \cdot \mathbf{E}(\Omega - \pi/2) \tag{6}$$

Again, the constants of proportionality in (5) and (6) are taken to be equal. The measured output voltage is the sum of V^a and V^t, and from (3), (5)

and (6) one obtains

$$
\begin{aligned}
V &\equiv V^a + V^t \qquad (7)\\
&\propto (\mathbf{T}^a(\hat{k})\,\cos(\Omega) + \mathbf{T}^t(\hat{k})\,\sin(\Omega)) \cdot \hat{r}^a + \\
&\quad (\mathbf{T}^a(\hat{k})\,\sin(\Omega) - \mathbf{T}^t(\hat{k})\,\cos(\Omega)) \cdot \hat{r}^t \\
&= (\mathbf{T}^a(\hat{k}) \cdot \hat{r}^a - \mathbf{T}^t(\hat{k}) \cdot \hat{r}^t)\,\cos(\Omega) + (\mathbf{T}^t(\hat{k}) \cdot \hat{r}^a + \mathbf{T}^a(\hat{k}) \cdot \hat{r}^t)\,\sin(\Omega)
\end{aligned}
$$

Using the relation (*Bronstein and Semendjajew*, 1981), the derivation is given in the appendix,

$$a\,\sin(\Omega) + b\,\cos(\Omega) = A\,\cos(\Omega - \Phi) \qquad (8)$$

with

$$
\begin{aligned}
A &\equiv \sqrt{a^2 + b^2} \qquad (9)\\
\Phi &\equiv \mathrm{arctan2}(a, b)
\end{aligned}
$$

the phase delay of the measured voltage V (7) with respect to the electric field transmitted by the aligned dipole (1) is

$$\Phi = \mathrm{arctan2}\left(\mathbf{T}^t(\hat{k}) \cdot \hat{r}^a + \mathbf{T}^a(\hat{k}) \cdot \hat{r}^t, \mathbf{T}^a(\hat{k}) \cdot \hat{r}^a - \mathbf{T}^t(\hat{k}) \cdot \hat{r}^t\right) \qquad (10)$$

with $\mathbf{T}^a(\hat{k})$ and $\mathbf{T}^t(\hat{k})$ being defined by (4). Φ is the amount of carrier phase wind-up for transmitter and receiver antenna orientations $\hat{t}^a, \hat{t}^t$ and $\hat{r}^a, \hat{r}^t$. Here, $\mathrm{arctan2}(a, b)$ denotes the four-quadrant arctangent

$$\mathrm{arctan2}(a, b) \equiv \begin{cases} \mathrm{sgn}(a)\,\arctan\left|\frac{a}{b}\right| & : \quad b > 0 \\ \mathrm{sgn}(a)\,\frac{\pi}{2} & : \quad b = 0 \\ \mathrm{sgn}(a)\,\left(\pi - \arctan\left|\frac{a}{b}\right|\right) & : \quad b < 0 \end{cases} \qquad (11)$$

and the sign function is defined by

$$\mathrm{sgn}(a) \equiv \begin{cases} 1 & : \quad a > 0 \\ 0 & : \quad a = 0 \\ -1 & : \quad a < 0 \end{cases} . \tag{12}$$

Equation (10) is easily modified for a LHCP receiver antenna by changing the phase offset sign in (6). The factor $\mathbf{E}(\Omega - \pi/2)$ is replaced by $\mathbf{E}(\Omega + \pi/2)$ and the corresponding carrier phase wind-up value Φ_{L} is

$$\Phi_{\mathrm{L}} = \mathrm{arctan2}\left(\mathbf{T}^t(\hat{k}) \cdot \hat{r}^a - \mathbf{T}^a(\hat{k}) \cdot \hat{r}^t, \mathbf{T}^a(\hat{k}) \cdot \hat{r}^a + \mathbf{T}^t(\hat{k}) \cdot \hat{r}^t\right) \tag{13}$$

Alternatively, equation (13) is obtained directly from (10) by reversing the direction of the transverse receiver dipole, $\hat{r}^t$.

For reference, the results obtained by *Wu et al.* (1993) for a RHCP receiver antenna are quoted. Under the assumption that the transmitted signal is in a pure RHCP state (equation (3) in *Wu et al.* (1993)), they show that the carrier phase wind-up is given by

$$\tilde{\Phi} = \mathrm{sgn}(\zeta) \arccos\left(\frac{\mathbf{D} \cdot \mathbf{D}'}{|\mathbf{D}|\,|\mathbf{D}'|}\right) \tag{14}$$

(equation (30) in *Wu et al.* (1993)). Here, $\mathbf{D}$, $\mathbf{D}'$ and ζ are defined as

$$\begin{aligned} \mathbf{D}' &\equiv \hat{t}^a - \hat{k}\left(\hat{k} \cdot \hat{t}^a\right) - \hat{k} \times \hat{t}^t \\ \mathbf{D} &\equiv \hat{r}^a - \hat{k}\left(\hat{k} \cdot \hat{r}^a\right) + \hat{k} \times \hat{r}^t \\ \zeta &\equiv \hat{k} \cdot (\mathbf{D}' \times \mathbf{D}) \end{aligned} \tag{15}$$

Equations (10) and (14) are not identical; simulation results described in section 3, however, indicate that the differences between $\tilde{\Phi}$ and Φ for realistic

antenna geometries are on the order of a few mrad (about 0.1 mm in terms of phase path at L-band frequencies). The assumption by *Wu et al.* (1993) of pure RHCP transmitter signals is therefore well justified. Moreover, if the boresight vectors of the transmitter and receiver antenna lie in one plane, equations (10) and (14) are in fact equivalent as will be shown in the appendix. This condition is met for static ground-based receivers with their antennas' boresights pointing towards the zenith.

2.2 Phase Wind-up for Coherently Reflected Rays

In this section a signal is considered which is transmitted by a crossed dipole and coherently reflected from a plane, mirror-like surface at an incidence angle θ (e.g., *Anderson*, 2000; *Treuhaft et al.*, 2001; *Martín-Neira et al.*, 2001; *Cardellach et al.*, 2006). In the following, incoherent signal components in the reflected signal are not taken into account. The Fresnel reflection coefficients (*Hecht and Zajac*, 1997; *Born and Wolf*, 1980)

$$\begin{aligned} r_{\parallel} &= \frac{n^2\,\cos\theta - \sqrt{n^2 - \sin\theta}}{n^2\,\cos\theta + \sqrt{n^2 - \sin\theta}} \\ r_{\perp} &= \frac{\cos\theta - \sqrt{n^2 - \sin\theta}}{\cos\theta + \sqrt{n^2 - \sin\theta}} \end{aligned} \tag{16}$$

relate the electric field amplitudes of the incoming signal (superscript i), $E_{\parallel}^{(i)}$ and $E_{\perp}^{(i)}$, to the amplitudes of the reflected signal (superscript o),

$$\begin{aligned} E_{\parallel}^{(o)} &\equiv r_{\parallel}\, E_{\parallel}^{(i)} \\ E_{\perp}^{(o)} &\equiv r_{\perp}\, E_{\perp}^{(i)} \end{aligned} \tag{17}$$

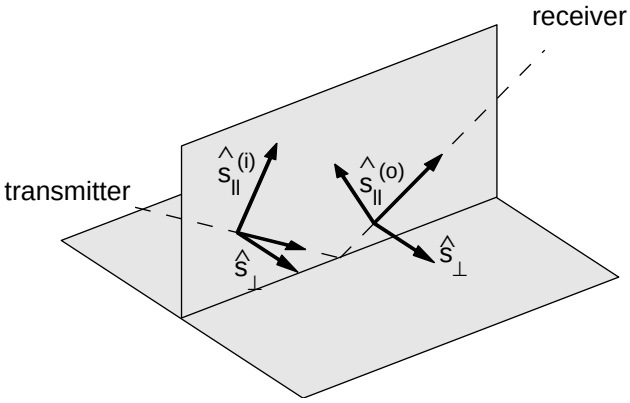

Fig. 3 Coordinate systems describing incoming and reflected ray and defining the signs in equation (16).

In (16), $n \equiv n_2/n_1$ denotes the ratio of the refractive index of the reflecting material, $n_2 = \sqrt{\epsilon_r} \equiv \sqrt{\epsilon/\epsilon_0}$, and the refractive index of air n_1. Here, ϵ_r is the real part of the relative dielectric constant. The signs in (16) correspond to the coordinate systems shown in Fig. 3 (*Hecht and Zajac*, 1997).

Again, the observed voltage is proportional to the electric field generated by the transmitting crossed dipoles at the location of the receiver antenna phase center (5,6). Using the Fresnel coefficients (16), the electric field vector of the reflected ray is determined from the electric field vector of the incoming ray by decomposing it into components parallel and perpendicular to the reflection plane (see (17) and Fig. 3).

The voltage recorded by the receiver antenna is thus given by

$$V_{\mathrm{rfl}} \propto (\mathbf{S}^a \cos(\Omega) + \mathbf{S}^t \sin(\Omega)) \cdot \hat{r}^a + \qquad (18)$$
$$(\mathbf{S}^a \sin(\Omega) - \mathbf{S}^t \cos(\Omega)) \cdot \hat{r}^t$$

$$= (\mathbf{S}^a \cdot \hat{r}^a - \mathbf{S}^t \cdot \hat{r}^t)\, \cos(\Omega) + (\mathbf{S}^t \cdot \hat{r}^a + \mathbf{S}^a \cdot \hat{r}^t)\, \sin(\Omega)$$

with the notation

$$\begin{aligned} \mathbf{S}^a &\equiv r_\parallel \left(\mathbf{T}^a(\hat{k}^{(i)}) \cdot \hat{s}_\parallel^{(i)}\right) \hat{s}_\parallel^{(o)} + r_\perp \left(\mathbf{T}^a(\hat{k}^{(i)}) \cdot \hat{s}_\perp\right) \hat{s}_\perp \\ \mathbf{S}^t &\equiv r_\parallel \left(\mathbf{T}^t(\hat{k}^{(i)}) \cdot \hat{s}_\parallel^{(i)}\right) \hat{s}_\parallel^{(o)} + r_\perp \left(\mathbf{T}^t(\hat{k}^{(i)}) \cdot \hat{s}_\perp\right) \hat{s}_\perp \end{aligned} \tag{19}$$

Here, $\mathbf{T}^a(\hat{k}^{(i)}) \cdot \hat{s}_\parallel^{(i)}$ and $\mathbf{T}^a(\hat{k}^{(i)}) \cdot \hat{s}_\perp$ are the amplitudes of the parallel and perpendicular components of the incoming electric field, respectively, which is generated by the aligned dipole (superscript a). Furthermore, $r_\parallel \left(\mathbf{T}^a(\hat{k}^{(i)}) \cdot \hat{s}_\parallel^{(i)}\right) \hat{s}_\parallel^{(o)}$ and $r_\perp \left(\mathbf{T}^a(\hat{k}^{(i)}) \cdot \hat{s}_\perp\right) \hat{s}_\perp$ are the parallel and perpendicular components of the reflected field, respectively. The phase wind-up of the reflected ray Φ^{rfl}, accordingly, is given by

$$\Phi^{\mathrm{rfl}} = \mathrm{arctan2}\left(\mathbf{S}^t \cdot \hat{r}^a + \mathbf{S}^a \cdot \hat{r}^t, \mathbf{S}^a \cdot \hat{r}^a - \mathbf{S}^t \cdot \hat{r}^t\right) \tag{20}$$

with $\mathbf{S}^a$ and $\mathbf{S}^t$ defined by (19). Analogous to (13), the corresponding wind-up value observed by a LHCP antenna is

$$\Phi_{\mathrm{L}}^{\mathrm{rfl}} = \mathrm{arctan2}\left(\mathbf{S}^t \cdot \hat{r}^a - \mathbf{S}^a \cdot \hat{r}^t, \mathbf{S}^a \cdot \hat{r}^a + \mathbf{S}^t \cdot \hat{r}^t\right) \tag{21}$$

As an aside, we note that the incoming ray's wave direction $\hat{k}^{(i)}$ closely matches the direct ray's direction vector $\hat{k}$, since the distance between reflection point and receiver generally is much smaller than the distance between receiver and GPS satellite and, therefore, $\mathbf{T}^a(\hat{k}^{(i)}) \approx \mathbf{T}^a(\hat{k})$ and $\mathbf{T}^t(\hat{k}^{(i)}) \approx \mathbf{T}^t(\hat{k})$.

2.3 Signal Intensities in Direct and Reflected Rays

Equations (8) and (9) also allow for estimating the relative signal amplitudes observed by RHCP and LHCP antennas. For the direct ray, the ratio of the RHCP and LHCP power levels is given by

$$R_{\mathrm{drct}}^{\mathrm{R/L}} = \frac{\left(\mathbf{T}^t(\hat{k}) \cdot \hat{r}^a + \mathbf{T}^a(\hat{k}) \cdot \hat{r}^t\right)^2 + \left(\mathbf{T}^a(\hat{k}) \cdot \hat{r}^a - \mathbf{T}^t(\hat{k}) \cdot \hat{r}^t\right)^2}{\left(\mathbf{T}^t(\hat{k}) \cdot \hat{r}^a - \mathbf{T}^a(\hat{k}) \cdot \hat{r}^t\right)^2 + \left(\mathbf{T}^a(\hat{k}) \cdot \hat{r}^a + \mathbf{T}^t(\hat{k}) \cdot \hat{r}^t\right)^2} \quad (22)$$

Similarly, the corresponding ratio for the reflected ray is

$$R_{\mathrm{rfl}}^{\mathrm{R/L}} = \frac{\left(\mathbf{S}^t \cdot \hat{r}^a + \mathbf{S}^a \cdot \hat{r}^t\right)^2 + \left(\mathbf{S}^a \cdot \hat{r}^a - \mathbf{S}^t \cdot \hat{r}^t\right)^2}{\left(\mathbf{S}^t \cdot \hat{r}^a - \mathbf{S}^a \cdot \hat{r}^t\right)^2 + \left(\mathbf{S}^a \cdot \hat{r}^a + \mathbf{S}^t \cdot \hat{r}^t\right)^2} \quad (23)$$

Section 3 provides example profiles for $R_{\mathrm{drct}}^{\mathrm{R/L}}$ and $R_{\mathrm{rfl}}^{\mathrm{R/L}}$ which were derived from simulated measurements.

3 Discussion

In the following, carrier phase wind-up corrections calculated from the analytic formulas are discussed on the basis of simulated GPS observations. The simulated signal is transmitted by GPS satellite PRN 17 on 17 July 2007 between 13 h and 17 h GPS time and recorded by a receiver located at the mountain top of Fahrenberg (47.617°N, 11.315°E, 1625 m above sea level). The corresponding sky trace of PRN 17 is shown in Fig. 4. For simplicity, the simulation assumes straight-line ray propagation and does not take into account phase delays induced by the ionosphere or neutral atmosphere.

The ground-based receiver antenna (boresight direction $\hat{r}^b$) is oriented towards East at an azimuth angle of +90° and at zenith angles of 0°, 45°

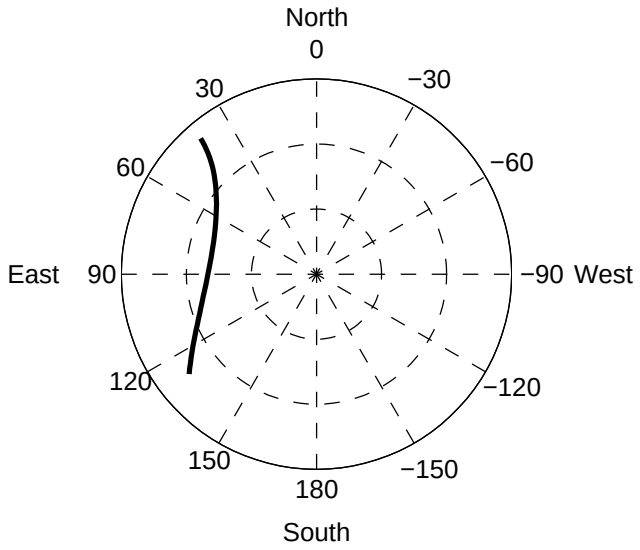

Fig. 4 GPS satellite sky trace for PRN 17 on 17 July 2007. The trace begins at 13 h in the South-East and ends at 17 h GPS time.

and 90°. The zenith angle is the angle between $\hat{r}^b$ and the zenith direction. The orientation vector $\hat{r}^a$ is aligned with respect to the azimuth direction. On the transmitter side, the antenna boresight $\hat{t}^b$ points to the center of the Earth and $\hat{t}^a$ is assumed to lie in the plane defined by $\hat{t}^b$ and the Earth-Sun line (*Bar-Sever*, 1996).

The simulation results are presented in terms of the phase path wind-up Λ and Λ_{rfl}

$$\Lambda \equiv \frac{\lambda}{2\pi}\,\Phi \qquad (24)$$
$$\Lambda_{\mathrm{rfl}} \equiv \frac{\lambda}{2\pi}\,\Phi^{\mathrm{rfl}}$$

where $\lambda \approx 19$ cm denotes the GPS L1 carrier signal's wavelength. The resulting phase path wind-up for the direct ray is shown in Fig. 5. The

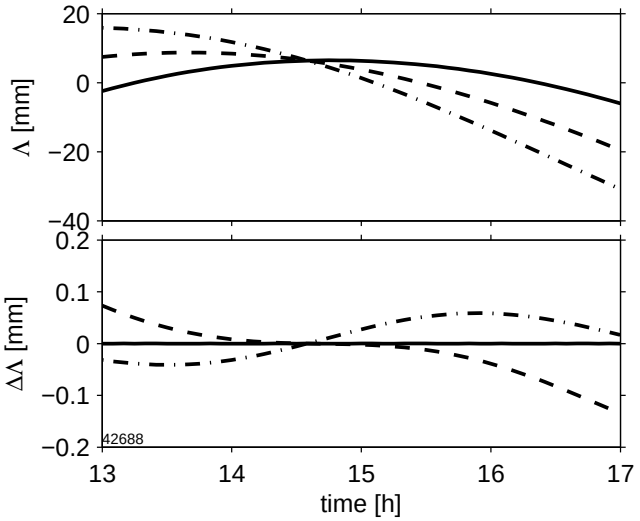

Fig. 5 Top: Simulated wind-up phase paths for PRN 17 on 17 July 2007 at the Fahrenberg measurement site (Fig. 4). The wind-up phase paths are derived from (10) for a receiver antenna azimuth angle of +90° and zenith angles of 0° (solid line), 45° (dashed) and 90° (dashed-dotted).

Bottom: Difference between wind-up phase path derived from equations (14) and (10) for zenith angles of 0° (solid line), 45° (dashed) and 90° (dashed-dotted). At 0° the two profiles are identical and the difference vanishes.

difference

$$\Delta\Lambda \equiv \frac{\lambda}{2\pi}\,(\tilde{\Phi} - \Phi) \tag{25}$$

vanishes for a zenith-oriented receiver antenna. However, for a zenith angle of 45° $\Delta\Lambda$ may reach values of up to 0.1 mm.

The simulated measurements also include a GPS reflectometry component with signals coherently reflected from the Walchensee lake surface about 824 m below the receiver location. The coherent reflection process

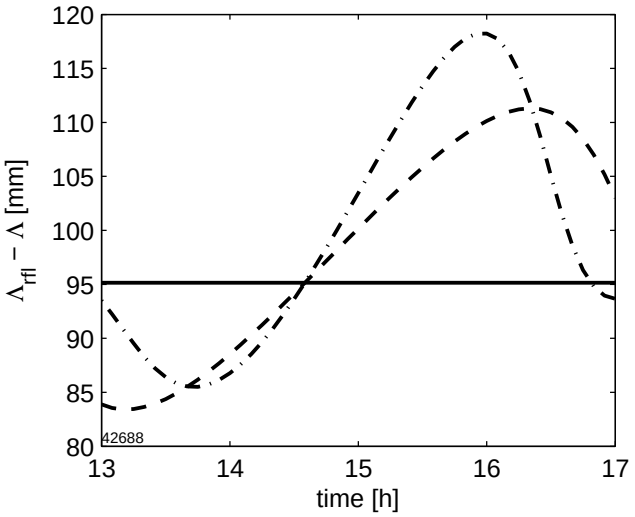

Fig. 6 The difference between the phase path wind-up of reflected and direct ray at the Fahrenberg measurement site. The simulated measurement is performed for PRN 17 on 17 July 2007 using receiver antenna zenith angles of 0° (solid line), 45° (dashed) and 90° (dashed-dotted) and an antenna azimuth angle of +90°.

is modelled according to (16) with a relative dielectric constant of water $\epsilon_r \equiv \epsilon/\epsilon_0 = 85.64$ and a refractive index of air 1.0004.

The difference in phase path wind-up for reflected and direct ray, $\Lambda_{\mathrm{rfl}} - \Lambda$, is shown in Fig. 6 for three receiver antenna zenith angles. For a zenith-pointing antenna, no dependence of $\Lambda_{\mathrm{rfl}} - \Lambda$ on antenna orientations is observed. However, for non-zero antenna zenith angles the phase path wind-up difference $\Lambda_{\mathrm{rfl}} - \Lambda$ may reach several centimeters and needs to be corrected for in reflectometry data analyses.

Finally, RHCP-to-LHCP power ratios are plotted in Fig. 7. The top panel shows the ratio $R_{\mathrm{drct}}^{\mathrm{R/L}}$ corresponding to the data set plotted in Fig. 5.

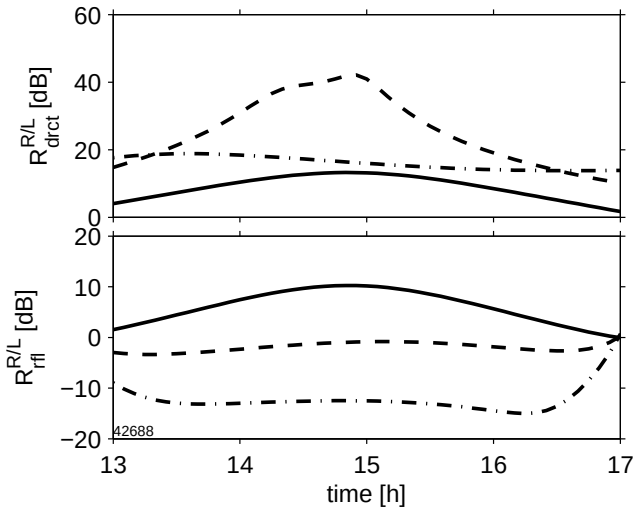

Fig. 7 Top: Power level ratio of RHCP to LHCP component (direct ray) for receiver antenna zenith angles of 0° (solid line), 45° (dashed) and 90° (dashed-dotted).

Bottom: Same as above, however, for the reflected ray.

For all three zenith angles $R^{\mathrm{R/L}}_{\mathrm{drct}}$ is positive indicating that the RHCP dominates the LHCP component. For a vertical pointing antenna $R^{\mathrm{R/L}}_{\mathrm{drct}}$ is smaller compared to the ratio at the other two antenna orientations, since the elevation of GPS satellite PRN 17 during the simulated measurement period is comparatively low and never exceeds 45° (Fig. 4). With a zenith angle of 45° (dashed line) at around 15 h GPS time, the receiver antenna boresight almost directly points towards the transmitter increasing $R^{\mathrm{R/L}}_{\mathrm{drct}}$ to more than 40 dB. For the reflected ray, on the other hand, the LHCP component dominates the RHCP component by about 10 dB if the antenna points towards to horizon (zenith angle of 90°, Fig. 7, bottom panel), whereas at 45° both

components are at about the same level. Thus, in the design of reflectometry experiments the antenna polarization type and orientation needs to be carefully selected.

Note that these considerations apply to the crossed dipole antenna model. The RHCP-to-LHCP power level ratios observed with real GPS antennas may differ significantly from the simulated data shown in Fig. 7.

4 Conclusions

An analytical expression for the carrier phase wind-up correction is derived which generalizes a well-known result derived by *Wu et al.* (1993). If the transmitter and receiver antennas' boresight directions lie in one plane the two formulae are equivalent. This condition is met in most ground-based applications with static receivers and antenna boresight directions pointing towards the zenith. For arbitrary orientations the expected deviations are in the sub-millimeter range. Carrier phase wind-up is a significant correction in GPS reflectometry. Using simulated measurements it is shown that the observed differences between direct and reflected ray phase path wind-up may reach up to several centimeters.

Acknowledgments

Helpful comments and suggestions by my colleagues at GFZ, Antonio Rius (IEEC, Barcelona) and an anonymous reviewer are gratefully acknowledged.

References

Anderson, K. D. (2000), Determination of water level and tides using interferometric observations of GPS signals, *J. Atmos. Ocean. Tech.*, *17*(8), 1118–1127, doi:10.1175/1520-0426.

Bar-Sever, Y. E. (1996), A new model for GPS yaw attitude, *Journal of Geodesy*, *70*(11), 714–723.

Beutler, G., et al. (2007), Bernese GPS software version 5.0, *Tech. rep.*, Astronomical Institute, University of Bern.

Born, M., and E. Wolf (1980), *Principles of Optics*, Pergamon Press, Oxford.

Bronstein, I. N., and K. A. Semendjajew (1981), *Taschenbuch der Mathematik*, Verlag Harri Deutsch, Thun.

Cardellach, E., S. Ribó, and A. Rius (2006), Technical note on polarimetric phase interferometry (POPI), *Tech. Rep. http://arxiv.org/abs/physics/0606099*.

García-Fernández, M., M. Markgraf, and O. Montenbruck (2008), Spin rate estimation of sounding rockets using GPS wind-up, *GPS Solutions*, *12*(3), 155–161.

Hecht, E., and A. Zajac (1997), *Optics*, Addison Wesley, Reading, MA.

Jackson, J. D. (1999), *Classical Electrodynamics*, John Wiley & Sons, Inc., New York.

Kim, D., L. Serrano, and R. Langley (2006), Phase wind-up analysis: Assessing real-time kinematic performance, *GPS World*, *17*(9), 58–64.

Martín-Neira, M., M. Caparrini, J. Font-Rosello, S. Lannelongue, and C. S. Vallmitjana (2001), The PARIS concept: An experimental demonstration of sea surface altimetry using GPS reflected signals, *IEEE Trans. Geosci. Remote Sensing*, *39*(1), 142–150.

Misra, P., and P. Enge (2006), *Global Positioning System: Signals, Measurements, and Performance*, Ganga-Jamuna Press, Lincoln, MA 01773, USA.

Montenbruck, O., M. García-Fernández, Y. Yoon, S. Schön, and A. Jäggi (2008), Antenna phase center calibration for precise positioning of LEO satellites, *GPS Solutions*, *12*, publ. online, doi:10.1007/s10291-008-0094-z.

Schmid, R., P. Steigenberger, G. Gendt, M. Ge, and M. Rothacher (2007), Generation of a consistent absolute phase-center correction model for GPS receiver and satellite antennas, *Journal of Geodesy*, *81*(12), 781–798.

Tetewsky, A. K., and F. E. Mullen (1997), Carrier phase wrap-up induced by rotating GPS antennas, *GPS World*, *8*(2), 51–57.

Treuhaft, R. N., S. T. Lowe, C. Zuffada, and Y. Chao (2001), 2-cm GPS altimetry over Crater lake, *Geophys. Res. Lett.*, *22*(23), 4343–4346.

Wu, J. T., S. C. Wu, G. A. Hajj, W. I. Bertiger, and S. M. Lichten (1993), Effects of antenna orientation on GPS carrier phase, *Manuscripta Geodaetica*, *18*(2), 91–98.

5 Appendix

In the following we first show that the phase wind-up value derived from (10) is identical to the value derived using (14) provided that the transmitter and receiver antenna boresight vectors $\hat{t}^b$ and $\hat{r}^b$ lie in one plane. We then derive (8).

The unit wave vector $\hat{k}$ can then be written as a linear combination of $\hat{t}^b$ and $\hat{r}^b$

$$\hat{k} = \alpha\,\hat{t}^b + \beta\,\hat{r}^b \tag{26}$$

where it is assumed that $\hat{t}^b$ and $\hat{r}^b$ are not collinear. We define nine parameters a, b, c, d, A, B, C, D and Δ by

$$\mathcal{R} \equiv \begin{pmatrix} \hat{t}^a \cdot \hat{r}^a & \hat{t}^a \cdot \hat{r}^t & \hat{t}^a \cdot \hat{r}^b \\ \hat{t}^t \cdot \hat{r}^a & \hat{t}^t \cdot \hat{r}^t & \hat{t}^t \cdot \hat{r}^b \\ \hat{t}^b \cdot \hat{r}^a & \hat{t}^b \cdot \hat{r}^t & \hat{t}^b \cdot \hat{r}^b \end{pmatrix} \equiv \begin{pmatrix} a & c & A \\ b & d & B \\ C & D & \Delta \end{pmatrix} \tag{27}$$

noting that

$$\begin{aligned} \Delta &= \left(\hat{t}^a \times \hat{t}^t\right) \cdot \left(\hat{r}^a \times \hat{r}^t\right) \\ &= \left(\hat{t}^a \cdot \hat{r}^a\right)\,\left(\hat{t}^t \cdot \hat{r}^t\right) - \left(\hat{t}^t \cdot \hat{r}^a\right)\,\left(\hat{t}^a \cdot \hat{r}^t\right) \\ &= a\,d - b\,c\,. \end{aligned} \tag{28}$$

Since the vectors $[\hat{t}^a, \hat{t}^t, \hat{t}^b]$ and $[\hat{r}^a, \hat{r}^t, \hat{r}^b]$ can be regarded as bases of cartesian coordinate systems, the matrix $\mathcal{R}$ is orthonormal, i.e.

$$\begin{aligned} \sum_{k=1}^{3} \mathcal{R}_{ik}\,\mathcal{R}_{jk} &= \delta_{ij} \\ \sum_{k=1}^{3} \mathcal{R}_{ki}\,\mathcal{R}_{kj} &= \delta_{ij} \end{aligned} \tag{29}$$

with the Kronecker delta defined by

$$\delta_{ij} \equiv \begin{cases} 0 & : \quad i \neq j \\ 1 & : \quad i = j \end{cases} \tag{30}$$

For example, equation (29) translates into the following relations which will be used later

$$c\,A + d\,B + D\,\Delta = 0 \tag{31}$$

$$a^2 + b^2 + C^2 = 1 \tag{32}$$

$$c^2 + d^2 + D^2 = 1 \tag{33}$$

$$a^2 + c^2 + A^2 = 1 \tag{34}$$

$$b^2 + d^2 + B^2 = 1 \tag{35}$$

$$C^2 + D^2 + \Delta^2 = 1 \tag{36}$$

From (26) and $|\hat{k}| = 1$ it follows that

$$\alpha^2 + \beta^2 + 2\,\alpha\,\beta\,\Delta = 1 \tag{37}$$

and equations (32), (33) and (36) yield

$$a^2 + b^2 + c^2 + d^2 = 1 + \Delta^2 \tag{38}$$

Equation (10) can now be re-written in terms of the parameters defined in (27),

$$\begin{aligned} \mathbf{T}^t(\hat{k}) \cdot \hat{r}^a &= \left(\left(\hat{k} \times \hat{t}^t \right) \times \hat{k} \right) \cdot \hat{r}^a \\ &= \left(\hat{t}^t - \hat{k} \left(\hat{k} \cdot \hat{t}^t \right) \right) \cdot \hat{r}^a \\ &= b - \alpha\,\beta\,B\,C \end{aligned} \tag{39}$$

Similarly, one obtains

$$\mathbf{T}^a(\hat{k}) \cdot \hat{r}^t = c - \alpha\,\beta\,A\,D \tag{40}$$

$$\mathbf{T}^a(\hat{k}) \cdot \hat{r}^a = a - \alpha\,\beta\,A\,C$$

$$\mathbf{T}^t(\hat{k}) \cdot \hat{r}^t = d - \alpha\,\beta\,B\,D$$

In the next step, the products $A\,D$, $B\,C$, $A\,C$ and $B\,D$ are expressed in terms of a, b, c and d. For example, by squaring (31), inserting (35), (34) and (33) and using (38) one obtains

$$\begin{aligned} A\,D &= \frac{1}{2\,c\,\Delta}\,\left(d^2\,(1-b^2-d^2) - c^2\,(1-a^2-c^2) - \Delta^2\,(1-c^2-d^2)\right) \\ &= \frac{1}{2\,c\,\Delta}\,\left(d^2\,(a^2+c^2-\Delta^2) - c^2\,(b^2+d^2-\Delta^2) - \Delta^2\,(1-c^2-d^2)\right) \\ &= \frac{1}{2\,c\,\Delta}\,\left(\Delta\,(a\,d+b\,c) - \Delta^2 + 2\,c^2\,\Delta^2\right) \\ &= b + c\,\Delta \end{aligned} \tag{41}$$

Similarly, for the remaining products one finds

$$B\,C = c + b\,\Delta \qquad A\,C = -d + a\,\Delta \qquad B\,D = -a + d\,\Delta \tag{42}$$

and (10) becomes

$$\Phi = \arctan2(b+c, a-d)$$

The corresponding expressions for (15) are

$$\begin{aligned} \mathbf{D}\cdot\mathbf{D}' &= a - d + \alpha\,\beta\,(B\,D - A\,C) + (\alpha-\beta)\,(a-d) \\ &= (a-d)\,(1+\alpha-\beta-\alpha\,\beta\,(1+\Delta)) \end{aligned} \tag{43}$$

$$|\mathbf{D}|^2 = \mathbf{D}\cdot\mathbf{D} = 2 - \alpha^2\,(C^2+D^2) - 2\,\alpha\,\Delta - 2\,\beta$$

$$= (1 - \alpha\,\Delta - \beta)^2$$

$$|\mathbf{D}'|^2 = \mathbf{D}' \cdot \mathbf{D}' = 2 - \beta^2\,(A^2 + B^2) + 2\,\beta\,\Delta + 2\,\alpha$$

$$= (1 + \alpha + \beta\,\Delta)^2$$

$$\zeta = \frac{1}{2}\,(b + c)\,(1 + \alpha - \beta)^2$$

using (26) and (37). Note that (14) and (43) imply

$$|\mathbf{D}| = 1 - \alpha\,\Delta - \beta \neq 0 \quad \text{and} \quad |\mathbf{D}'| = 1 + \alpha + \beta\,\Delta \neq 0\,. \tag{44}$$

Using (43) and (37), $\tilde{\Phi}$ is given by

$$\begin{aligned}\tilde{\Phi} &= \operatorname{sgn}(\zeta)\arccos\left(\frac{(a-d)\,(1+\alpha-\beta-\alpha\,\beta\,(1+\Delta))}{(1-\alpha\,\Delta-\beta)\,(1+\alpha+\beta\,\Delta)}\right) \\ &= \operatorname{sgn}(b+c)\arccos\left(\frac{a-d}{1-\Delta}\right)\end{aligned} \tag{45}$$

since

$$(1 - \alpha\,\Delta - \beta)\,(1 + \alpha + \beta\,\Delta) = (1 - \Delta)\,(1 + \alpha - \beta - \alpha\,\beta\,(1 + \Delta))\,. \tag{46}$$

In equation (45) $\operatorname{sgn}(\zeta)$ has been replaced by $\operatorname{sgn}(b + c)$ which is only admissible for $1 + \alpha - \beta \neq 0$. However, if $1 + \alpha - \beta = 0$ the rhs of (46) was identically zero (see (37)) contradicting (44).

With $\operatorname{arctan2}(\sqrt{1 - x^2}, x) = \arccos x$, where $-1 \leq x \leq +1$, one finds for $x \equiv (a - d)/(1 - \Delta)$ that $\sqrt{1 - x^2} = |b + c|/(1 - \Delta)$. Thus,

$$\begin{aligned}\tilde{\Phi} &= \operatorname{sgn}(b+c)\arccos\left(\frac{a-d}{1-\Delta}\right) \\ &= \operatorname{sgn}(b+c)\operatorname{arctan2}\left(\frac{|b+c|}{1-\Delta}, \frac{a-d}{1-\Delta}\right) \\ &= \operatorname{arctan2}(b+c, a-d) \\ &= \Phi\end{aligned} \tag{47}$$

concluding the proof that $\Phi = \tilde{\Phi}$ provided the transmitter and receiver antenna boresight vectors $\hat{t}^b$ and $\hat{r}^b$ lie in one plane.

Equation (8) is derived in the following way: with $\sin\Omega = (e^{i\Omega} - e^{-i\Omega})/(2i)$ and $\cos\Omega = (e^{i\Omega} + e^{-i\Omega})/2$ we find

$$\begin{aligned} a\,\sin\Omega + b\,\cos\Omega &= \left(\frac{a}{2i} + \frac{b}{2}\right) e^{i\Omega} + \left(-\frac{a}{2i} + \frac{b}{2}\right) e^{-i\Omega} \qquad (48) \\ &= \frac{1}{2}\,\sqrt{a^2+b^2}\,e^{-i\,\mathrm{arctan2}(a,b)}\,e^{i\Omega} + \\ &\quad \frac{1}{2}\,\sqrt{a^2+b^2}\,e^{i\,\mathrm{arctan2}(a,b)}\,e^{-i\Omega} \\ &= \sqrt{a^2+b^2}\,\cos(\Omega - \mathrm{arctan2}(a,b)) \end{aligned}$$